International Journal of Mechanics and Energy (IJME)
Vol. 1, Issue 3, 2013, ISSN: 2286-5845

Influence of wall boundary conditions on the 3D double diffusive convection and on the entropy generation

Kaouther Ghachem[1], Chamseddine Maatki, Lioua Kolsi, Mohamed Naceur Borjini, Habib Ben Aissia
Unité de Métrologie et de SystèmesEnergétiques, National School of Engineers of Monastir (ENIM), University of Monastir (UM),Route Ibn Al Jazzar, Monastir, 5030, TUNISIA,

Abstract: In this paper we study numerically the 3D double-diffusive natural convection in a cubic cavity. The main purpose of this paper is to study the effect of the modification of the boundary condition of the upper and down sides of a cubical cavity, on the flow and heat transfer in the one side and on the entropy generated on the other side. The flow is considered laminar and caused by the interaction of thermal energy and the chemical species diffusions. The governing equations of the problem, concentration, energy and momentum, are formulated using vector potential-vorticity formalism in its three-dimensional form, then solved by the finite volumes method. The Rayleigh number is fixed at $Ra=10^5$ and the effects of the buoyancy ratio is studied for opposed temperature and concentration gradients. The particular interest is focalized on the three-dimensional aspects and entropy generation.

Keywords: 3D cavity, entropy generation, natural convection, double diffusive

1. Introduction

During the past several decades, a large number of numerical investigations have been carried out on the steady-state natural convection in enclosure since De Vahl Davis [1] published his benchmark solutions about a differentially heated enclosure. Kim and Viskanta [4] performed numerical and experimental investigations on the steady-state conjugate conduction–convection in a square enclosure of conductive walls. They found that under certain configuration and with specific parameters selection, the existence of solid walls reduces the average temperature difference across the centered cavity and hence partially stabilizes the flow and weakens the natural convection heat transfer. Acharya and Tsang [5] investigated the effects of wall conduction and enclosure inclination. Their work showed that the heat transfer rate decreases with decreasing conductivity ratio and increasing wall thickness, while it is hardly affected by the enclosure inclination since in their study the wall thickness accounts for 10–25% of the enclosure length and the heat transfer is conduction-dominated. Mobedi[16] focused on the natural convection in a square enclosure with horizontal conductive walls; the results showed that the heat transfer rate is also affected by the combination of Rayleigh number and the thermal conductivity ratio.

[1] Corresponding author:kaouther Ghachem
Email: kaouther_ghachem@yahoo.fr

For the situation of single convection in both two and three-dimensional enclosures, many works include the effect of imperfectly insulated horizontal walls [6, 13]. The investigation of Leonardi et al. [14] shows that the 3-D flow structures depend strongly on the thermal boundary conditions. As a consequence, the overall heat flux is influenced.

Double diffusive natural convection is generated by buoyancy due simultaneous to temperature and concentration gradients. This mode of heat and mass transfer has aspecific interest in several fields such as drying processes, crystal growth processes, solar desalination, etc. Principles of thermo solutal convection are well documented by Bejan [2]. In the problem of double diffusion, two physical configurations may be encountered. On the first, heat and mass gradients are imposed horizontally along the enclosure [6, 7, and 13], while in the second, heat and mass gradients are imposed vertically [11]. In both cases, the gradients may be aiding or opposing each other's. The main objectives of these works are usually the numerical study of resulting flow structures for several dimensionless parameters. The most important and interesting convective phenomena occur at the transiting between thermally and solutal driven flows. As discussed by Nishimura et al. [13], this transition takes place when the buoyancy ratio isclose to 1. A few of studies are interested in the 3D double diffusive natural convection. Sezai and Mohamed [15] studied thermosolutal natural convection in a cubic enclosure subject to horizontal and opposing gradients of heat and solute, they indicated that the double-diffusive flow in enclosures was strictly three-dimensional for a

certain ranges of Rayleigh number, Lewis number and buoyancy ratio respectively. The same configuration was studied by Abidi et al. [16] but with heat and mass diffusive horizontal walls. They mentioned that the effect of the heat and mass diffusive walls was found to reduce the transverse velocity for the thermal buoyancy-dominated regime and to increase it considerably for the compositional buoyancy-dominated regime. Ghachem et al. [18] studied numerically double diffusive natural convection and entropy generation in three-dimensional solar dryer with an aspect ratio equal to 2. They found that the variation of the buoyancy ratio affects significantly the isotherms distributions, iso-concentrations and the flow structure. Particularly for N=1, the flow is completely three-dimensional. Besides, they found that all kinds of entropies generation present a minimum for N=1. This result is due to the competition between thermal and compositional forces. These entropies rise considerably when N grows. On the one hand, the maximum of Bejan number is found for N=1 witch indicated the domination of heat and mass irreversibilities. Outside, friction irreversibilties are largely dominant. On the other hand, distribution of Local Nusselt numbers changes with changing buoyancy ratio and take a complex structure for N=1.

Costa [12] studied numerically the double-diffusive natural convection in a square enclosure with horizontal heat and mass diffusive walls. The main objectives of his study were the formulation of a mathematical model for this problem and the analysis of the effects of the heat and mass transfer participating walls. His analysis was restricted to particular combinations of the governing dimensionless parameters for a cavity filled with moist air.

This study addresses the effect of the change of the upper and lower side's boundary conditions of a cubic cavity, on the heat and mass transfer on the one hand and on the entropy created on the other hand.

2. Nomenclature

C	Dimensionless concentration $C=((C'-C_l')/(C_h'-C_l'))$
D	Mass diffusivity
Gr	Grashof number
g	Acceleration of gravity
H	Enclosure heigh
k	Thermal conductivity
Le	Lewis Number
N	buoyancy ratio
Pr	Prandtl number
$\vec{q}'$	Heat flux vector
Ra	Rayleigh number
Sc	Schmidt number
Sh	Sherwood number
S'_{gen}	generated entropy
t	dimensionless time ($t=t'.\alpha/l^2$)
T	dimensionless temperature $T=[(T'-T'_c)/(T'_h-T'_c)]$
T'_c	cold temperature
T'_h	hot temperature
$\vec{V}$	dimensionless velocity vector ($\vec{V}=\vec{V}'.l/\alpha$)
W	enclosure width

Greek symbols

α	Thermal diffusivity ($m^2.s^{-1}$)
β	Expansion coefficient ($m^3.kg^{-1}$)
Φ'	Dissipation function
ρ	Density
μ	Dynamic viscosity
ν	Kinematic viscosity
υ_0	Characteristic speed of fluid ($\upsilon_0=\alpha/l$)
$\vec{\psi}$	Dimensionless vector potential ($\vec{\psi}=\vec{\psi}'/\alpha$)
$\vec{\omega}$	Dimensionless vorticity ($\vec{\omega}=\vec{\omega}'.\alpha/l^2$)

Subscripts

c	compositional
t	Thermal
o	Initial
x, y, z	Cartesian coordinates

Superscript

'	Dimensional variable

3. Mathematical formulation

The geometry of the cubical cavity under analysis and the coordinate system are shown in Figure 1. The vertical sides walls (x=0 and x=1) are maintained at constant and uniform different levels of temperature and concentration, thus giving rise to three dimensional double diffusive natural-convection problem. However, the upper and down side walls (y=0 and y=1) are subject of different cases of boundary conditions studied later which are: adiabatic boundary conditions (case 1), uniform temperature (case 2), uniform concentration (case 3) and finally uniform temperature and concentration. The other faces (z=0 and z=1) are considered adiabatic.

The fluid contained in the cavity is assumed incompressible and the flow follows the approximation of Boussinesq.

The governing equations that describing the double diffusive natural convection are the equations of continuity, of momentum, of energy and species diffusion:

$$\nabla.\vec{V}'=0 \tag{1}$$

$$\frac{\partial\vec{V}'}{\partial t'}+(\vec{V}'.\vec{\nabla})\vec{V}'=-\frac{1}{\rho}\vec{\nabla}P'+\nu\Delta\vec{V}'+\beta_t(T'-T_0)\vec{g}+\beta_c(C'-C_0)\vec{g} \tag{2}$$

$$\frac{\partial T'}{\partial t'}+\vec{V}'.\nabla T'=\alpha\nabla^2T' \tag{3}$$

$$\frac{\partial C'}{\partial t'} + \vec{V}'.\nabla C' = D\nabla^2 C' \quad (4)$$

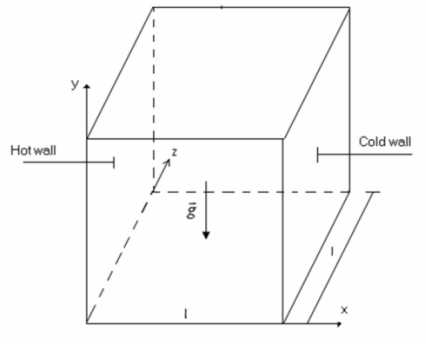

Figure 1.Physical model

In order to eliminate the pressure term, which is delicate to treat, the numerical method used in this work is based on the vorticity-vector potential formalism $(\vec{\psi} - \vec{\omega})$. For this, one applies the rotational to the equation of momentum. The vector potential and the vorticity are, respectively, defined by the two following relations:

$$\vec{\omega}' = \vec{\nabla} \times \vec{V}' \quad \text{and} \quad \vec{V}' = \vec{\nabla} \times \vec{\psi}' \quad (5)$$

Based on the dimensionless variables the governing equations can be written as:

$$-\vec{\omega} = \nabla^2 \vec{\psi} \quad (6)$$

$$\frac{\partial \vec{\omega}}{\partial t} + (\vec{V}.\nabla)\vec{\omega} - (\vec{\omega}.\nabla)\vec{V} = \Delta\vec{\omega} + Ra.\Pr.\left[\frac{\partial T}{\partial z} - N\frac{\partial C}{\partial z};0;-\frac{\partial T}{\partial x} + N\frac{\partial C}{\partial x}\right] \quad (7)$$

$$\frac{\partial T}{\partial t} + \vec{V}.\nabla T = \nabla^2 T \quad (8)$$

$$\frac{\partial C}{\partial t} + \vec{V}.\nabla C = \frac{1}{Le}\nabla^2 C \quad (9)$$

With:
$$\Pr = \nu/\alpha \qquad Ra = \frac{g.\beta_t.W^3.(T_h^{'} - T_c^{'})}{\alpha.\nu}$$
$$N = \frac{\beta_c.(C_h^{'} - C_l^{'})}{\beta_t.(T_h^{'} - T_c^{'})} \qquad Le = \frac{\alpha}{D} = \frac{Sc}{\Pr}$$

The physical boundary conditions can be defined for all the variables, as follows:

Temperature
$T = 1$ at $x = 1$
$T = 0$ at $x = 0$
$\frac{\partial T}{\partial z} = 0$ at z=(0,1) adiabatic walls

Concentration:
$C = 1$ at $x = 1$
$C = 0$ at $x = 0$
$\frac{\partial C}{\partial z} = 0$ at z=(0,1) impermeablewalls

At y=(0,1) three cases areevoked:

Case 1 T=1 and $\frac{\partial C}{\partial y} = 0$

Case 2 $\frac{\partial T}{\partial y} = 0$ and C=1

Case 3: T=1 and C=1

Vorticity:
$\omega_x = 0 \quad \omega_y = -\frac{\partial V_z}{\partial x} \quad \omega_z = \frac{\partial V_y}{\partial x}$ at x=(0,1)

$\omega_x = \frac{\partial V_z}{\partial y} \quad \omega_y = 0 \quad \omega_z = -\frac{\partial V_x}{\partial y}$ at y=(0,1)

$\omega_x = -\frac{\partial V_y}{\partial z} \quad \omega_y = \frac{\partial V_x}{\partial z} \quad \omega_z = 0$ at z=(0,1)

Vector potential
$\frac{\partial \psi_x}{\partial x} = \psi_y = \psi_z = 0$ at x=(0,1)
$\psi_x = \frac{\partial \psi_y}{\partial y} = \psi_z = 0$ at y=(0,1)
$\psi_x = \psi_y = \frac{\partial \psi_z}{\partial z} = 0$ at z=(0,1)

Velocity: $V_x = V_y = V_z = 0$ on all walls

The local entropy generation rate in a three-dimensional flow with single diffusing specie of concentration (C) can be written as [11]:

$$S'_{gen} = \left\{\frac{k}{T_0^2}\left[\left(\frac{\partial T'}{\partial x'}\right)^2 + \left(\frac{\partial T'}{\partial y'}\right)^2 + \left(\frac{\partial T'}{\partial z'}\right)^2\right]\right\} + \frac{\mu}{T_0}\left\{\begin{array}{l} 2\left[\left(\frac{\partial u'_1}{\partial x'}\right)^2 + \left(\frac{\partial u'_2}{\partial y'}\right)^2 + \left(\frac{\partial u'_3}{\partial z'}\right)^2\right] + \\ \left(\frac{\partial u'_2}{\partial x'} + \frac{\partial u'_1}{\partial y'}\right)^2 + \left(\frac{\partial u'_3}{\partial y'} + \frac{\partial u'_2}{\partial z'}\right)^2 + \left(\frac{\partial u'_1}{\partial z'} + \frac{\partial u'_3}{\partial x'}\right)^2 \end{array}\right\} + \left\{\begin{array}{l} \frac{RD}{C_0}\left[\left(\frac{\partial C'}{\partial x'}\right)^2 + \left(\frac{\partial C'}{\partial y'}\right)^2 + \left(\frac{\partial C'}{\partial z'}\right)^2\right] + \\ \frac{RD}{T_0}\left[\left(\frac{\partial T'}{\partial x'}\right)\left(\frac{\partial C'}{\partial x'}\right) + \left(\frac{\partial T'}{\partial y'}\right)\left(\frac{\partial C'}{\partial y'}\right) + \left(\frac{\partial T'}{\partial z'}\right)\left(\frac{\partial C'}{\partial z'}\right)\right] \end{array}\right\} \quad (10)$$

Where C_o and T_o are respectively the reference concentration and temperature. The dimensional form of the local entropy generation is as follow:

$$N_S = \left[\left(\frac{\partial T}{\partial x}\right)^2 + \left(\frac{\partial T}{\partial y}\right)^2 + \left(\frac{\partial T}{\partial z}\right)^2\right] + \varphi_1 \left\{ \begin{array}{l} 2\left[\left(\frac{\partial V_x}{\partial x}\right)^2 + \left(\frac{\partial V_y}{\partial y}\right)^2 + \left(\frac{\partial V_z}{\partial z}\right)^2\right] + \\ \left[\left(\frac{\partial V_y}{\partial x} + \frac{\partial V_x}{\partial y}\right)^2 + \left(\frac{\partial V_z}{\partial y} + \frac{\partial V_y}{\partial z}\right)^2 + \left(\frac{\partial V_x}{\partial z} + \frac{\partial V_z}{\partial x}\right)^2\right] \end{array} \right\} + \left\{ \begin{array}{l} \varphi_2\left[\left(\frac{\partial C}{\partial x}\right)^2 + \left(\frac{\partial C}{\partial y}\right)^2 + \left(\frac{\partial C}{\partial z}\right)^2\right] + \\ \varphi_3\left[\left(\frac{\partial T}{\partial x}\right)\left(\frac{\partial C}{\partial x}\right) + \left(\frac{\partial T}{\partial y}\right)\left(\frac{\partial C}{\partial y}\right) + \left(\frac{\partial T}{\partial z}\right)\left(\frac{\partial C}{\partial z}\right)\right] \end{array} \right\} \quad (11)$$

The first term of N_S represents the thermal irreversibility, it is noted $N_{S\text{-}th}$. The second term, $N_{S\text{-}fr}$, represents the viscous irreversibility and the third term, $N_{S\text{-}dif}$, represents the diffusive irreversibility. N_S gives a good idea on the profile and the distribution of the generated local dimensionless entropy. The total dimensionless generated entropy is written as follow:

$$S_{tot} = \int_v N_s dv = \frac{1}{v}\int_v \left(N_{s-th} + N_{s-fr} + N_{s-dif}\right) dv$$
$$S_{tot} = S_{th} + S_{fr} + S_{dif} \quad (12)$$

Bejan number (Be) is the ratio of heat and mass transfer irreversibility to the total irreversibility due to heat transfer and fluid friction:

$$Be = \frac{S_{th} + S_{dif}}{S_{th} + S_{fr} + S_{dif}} \quad (13)$$

Dimensionless irreversibility distribution ratios (φ_1, φ_2 and φ_3), are given by:

$$\varphi_1 = \frac{\mu\alpha^2 T_0}{L^2 k \Delta T^2} \quad \varphi_2 = \frac{RDT_0}{kC_0}\left[\frac{\Delta C'}{\Delta T'}\right] \quad \varphi_3 = \frac{RD}{k}\left[\frac{\Delta C'}{\Delta T'}\right] \quad (14)$$

For N = 0, there is no mass diffusion and we assume that the thermal and species diffusions are opposed.

4. Results and discussions

Numerical results are presented for Pr=0.71, Le=1.2 and Ra is fixed at 10^5. The buoyancy ratio is varied and three values are tested: N=0.5, N=1, N=2. The dimensionless irreversibility distribution ratios (φ_1, φ_2, φ_3) are fixed respectively at 10^{-4}, 0.5 and 10^{-2} [18].

Four boundary conditions will be treated in this section. The first one is the adiabatic boundary condition. In witch all the vertical and horizontal sides of the cavity will be adiabatic with the exception of the sides x=0 and x=1 which are subject of opposite gradient of temperature and concentration. This case will be considered as the standard configuration which is treated earlier by many authors [6, 10, and 15].

For the other cases of study, vertical sides (z=0 and z=1) will be maintained adiabatic. Although, the upper and down side are subject of different boundary conditions in the one side, they are maintained at uniform temperature, in the other side, they will be at uniform concentration and finally, they will be at uniform temperature and concentration. Two aspects will be discussed, namely: the flow structure behaviour and the heat and mass transfer and the entropy generation.

4.1. Flow structure and Heat and mass transfer

This section is devoted to the study of the flow structure in the one hand and to study the heat and mass transfer for each boundary condition tested, on the other hand.

4.1.1. Adiabatic boundary conditions

Figure 2(a) presents the projection of the velocity vector in the middle XY plan when N=0.5.

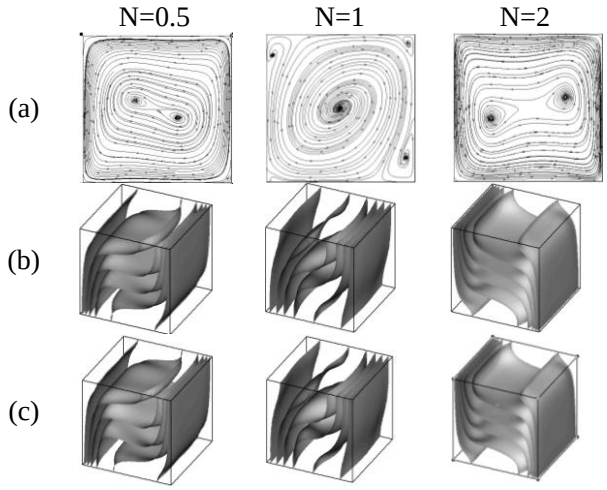

Figure 2 : projection of the velocity vector in the middle plan X-Y (a), iso-surfaces of temperature (b) and concentration (c) when the boundary conditions are adiabatic

Two thermal cells are turning in the same direction. Flow is thermal dominated. Figure 2 (b) and figure 2 (c) show the plots of isotherms and isoconcentrations. The first point to make is that the two plots of iso-surfaces of temperature and concentration have the same behavior. In fact, the thermal and solutal gradients are tightened near the down party of the hot wall and the top party of the cold wall. Moreover, vertical stratification is mentioned in the core of the cavity.

For N=1 (figure 2), the two thermal cells disappear and one central cell takes place. Also, three solutal cells appear: one is close to the top corner of the hot wall; however the two other are located at the top corner and at the down corner of the cold wall. Isothermal and isoconcentration profiles show that the thermal and the solutal gradients decrease.

When N=2, the flow becomes mono cellular and it is characterized by one cell with two inner vortexes turning counter the clockwise. The isothermal and is concentration profiles showed that the flow is solutal dominated by the increase of the stepper gradient near the top part of the hot wall and the down part of the cold wall.

4.1.2. Uniform temperature at the upper and down side

In this case of study, the side x=0 and y=(0, 1) are subject of uniform temperature (T=1) and the other walls (z= (0, 1)) are maintain adiabatic.

For N=0.5 (figure 3), the flow is characterized by one thermal cell situated in the center of the cavity and turning in the clockwise. Two solutal cells are localized simultaneously at the top and at the down corner of the hot wall and turning counter clockwise.

When N=0.85, two contra-rotative cells occupy the entire of the cavity.

For N=1, the flow is characterized also, by two contra-rotative cells with a dominance of the thermal cell. When N=2, the flow become with two solutal cells, one stretched to the hot wall and the other to the cold wall and turning in the opposite direction of the clockwise. One notes the existence of a small vortex near at the top corner of the cold wall.

The plots of isotherms show that the vertical stratification, appeared earlier when the boundary condition were adiabatic, becomes horizontal (figure 4.a). All the isothermals are connected to the top and down corner of the cold wall. When N=0.5, the distortion of these isotherms is deviated to the bottom of the cavity.

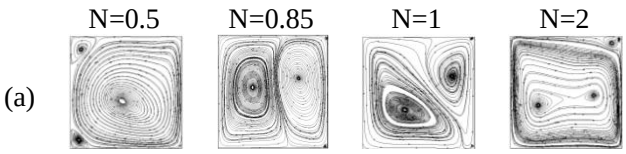

Figure 3. Projection of the velocity vector in the middle plan X-Y

By the increase of the N values, the horizontal stratification is more developed and becomes near the top wall of the cavity. The 3D aspect is more pronounced. Plots of isoconcentration still with the same aspect that those of the adiabatic boundary condition. However, one notes the existence of more distortion in the core of the cavity.

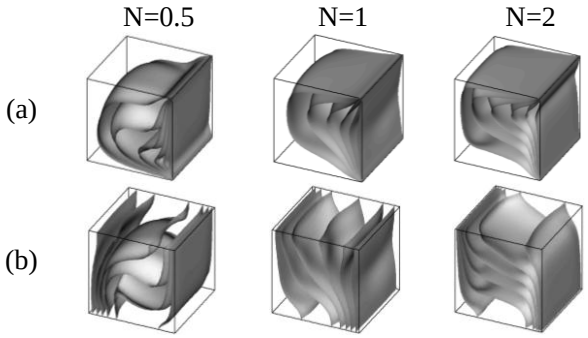

Figure 4. Iso-surfaces of temperature (b) and concentration (c) when the uniform temperature at the upper and down side

The stratification of the isoconcentration are inversed for N=1 with an increase of the solutal gradient near the down party of the cold wall. For N=2 the vertical stratification is more developed.

4.1.3.Uniform concentration at the upper and down side

Figure 5 presents the projection of the velocity vector in the middle plan X-Y for different values of buoyancy ratio and the iso-surfaces of temperature and concentration when the upper and down walls are at uniform concentration and adiabatic.

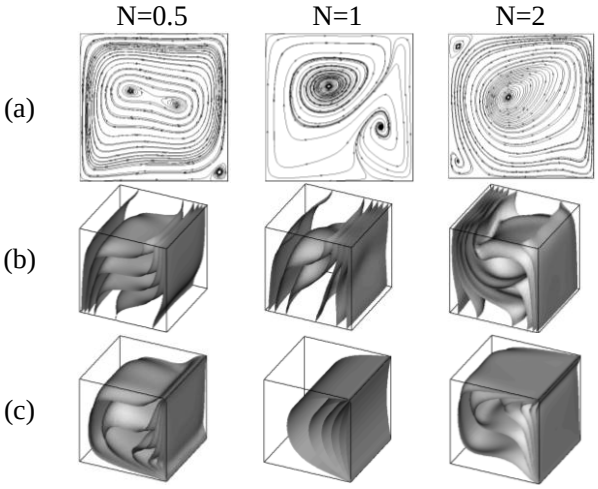

Figure 5. Projection of the velocity vector in the middle plan X-Y (a), iso-surfaces of temperature (b) and concentration (c) when the boundary conditions are uniform

When N=0.5, the flow is characterized by one cell with two inner vortexes which turning in the opposite sense. Furthermore, one solutal vortex appears in the down corner of the cold wall and turning in the clockwise. For N=1, two contra-rotative cells appear in the cavity. When N=2, one central cell takes place and two small vortex appear respectively at the top and down corner of the hot wall.

By analyzing the plots of isotherms, the most important remark is the appearance of a central stratification for N=2.
Moreover, the location of the stepper gradient is inversed witch mentioned the importance of the buoyancy forces.

4.1.4. Uniform temperature and concentration at the upper and down side

In this case, boundary conditions are simultaneously at uniform temperature and concentration in the upper and down walls of the cavity. Plots of isotherms and isoconcentration present similar profiles (figure 6). For N=0.5, the flow structure is characterized by one thermal central cell witch rotating in the clockwise. For N=1, the flow is characterized by two contra-rotative cells. The thermal cell is localized near the down corner of the hot wall although the solutal cell occupies the rest of the cavity.
By the increase of N value, two solutal cells appear and rotating in the same direction.

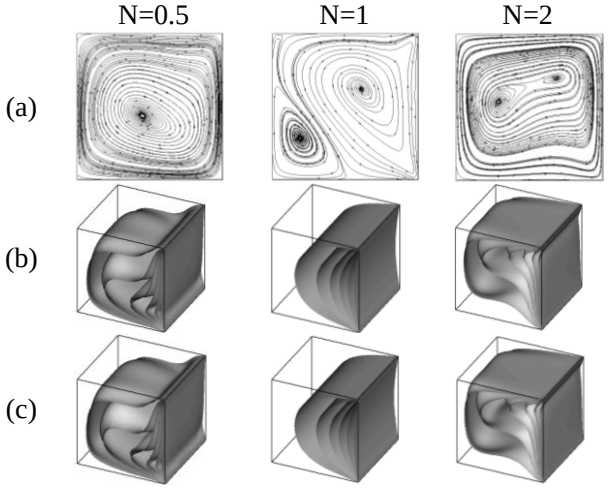

Figure 6. Projection of the velocity vector in the middle plan X-Y (a), iso-surfaces of temperature (b) and concentration (c) when the boundary conditions are at uniform temperature and concentration

4.2. Entropy generation

4.2.1. Adiabatic boundary conditions

Figure 7, presents the entropy generation when boundary conditions are adiabatic. Regardless The buoyancy ratio, thermal and solutal entropies are located near the active walls (figure 7 (a) and (b)).That said, when N=1, the contour of thermal entropy becomes close to the lower half of the hot wall and to the upper half of the cold wall. However, the solutal entropy is restricted to the bottom of the hot wall and upward from the cold wall and reaches a maximum equal to 40.876. When thermal and compositional forces are equals(N=1), the total generated entropy is distributed on the entire cavity and not localized near walls, which implies a suppression of boundary layer phenomenon met in other cases [18].

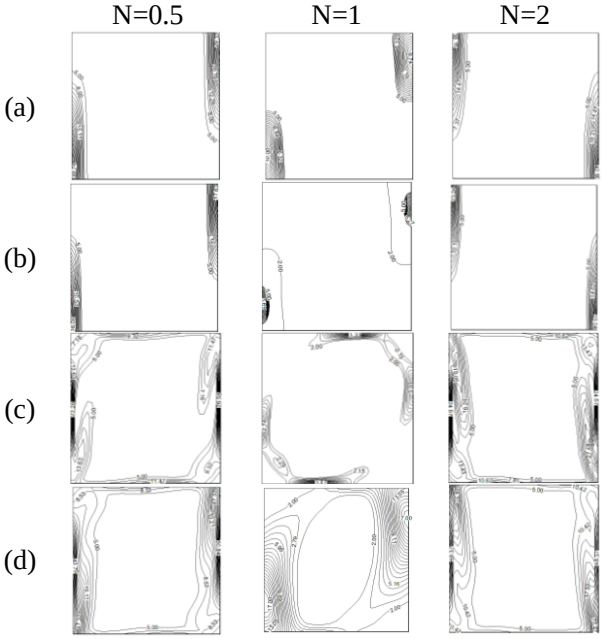

Figure 7. Entropies generation in the XY plan for different N when the boundary conditions are adiabatic; (a) thermal, (b) compositional; (c) friction and (d) total

4.2.2. Uniform temperature at the down at upper side of the cavity

For N=0.5, the maximum value of the thermal entropy evolves from 35.82, in the case of adiabatic boundary condition, to138.29inthis case of study.

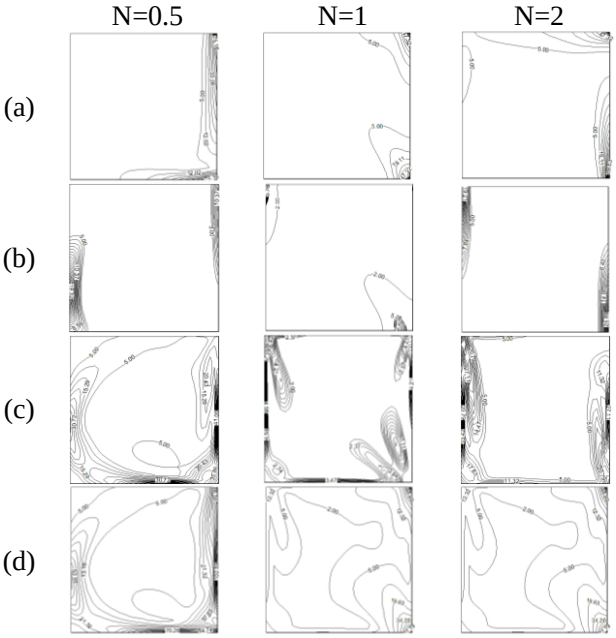

Figure 8. Entropies generation in the XY plan for different N when the boundary condition are at uniform temperature; (a) thermal , (b) compositional; (c) friction and (d) total

This Value of thermal entropy remains practically identical in the case where N= 1 and N = 2. Besides, contours of thermal entropy become localized on the one hand, between the upper parts of the cold wall and near the top wall. On the other hand, it is situated in the bottom corner of the cold walls. By the increase of N, these contours are spread throughout the top wall, the cold wall and a portion of the hot wall. The solutal entropy contours are closer to the active walls with a maximum value reaches 138.675 when the buoyancy ratio is equal to 2.

4.2.3. Uniform concentration at the upper and down boundary condition

In this case of study, the thermal entropy generation is close to the active wall for N=0.5 and N=2. However, it is spread in the entire cavity when the buoyancy ratio is equal to 1. The maximum value of the solutal entropy reaches height values: 141.438 for N=0.5, 139.93 for N=1 and 137.584 for N=2. When N=0.5, solutal entropy is close to the cold and bottom wall whereas N=2, it is closer to the cold and top wall of the cavity.

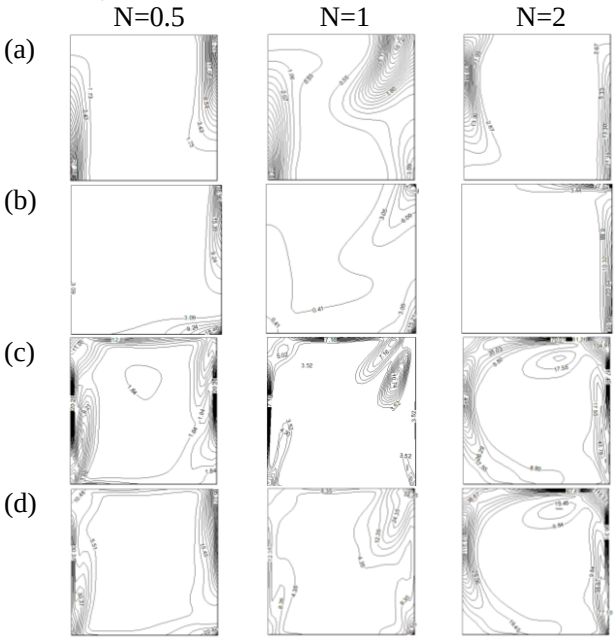

Figure 9. Entropies generation in the XY plan for different N when the boundary condition are at uniform concentration; (a) thermal , (b) compositional; (c) friction and (d) total

4.2.4. Uniform temperature and concentration at the upper and down boundary conditions

When N=0.5 (figure 10), the thermal and compositional entropy are located close to the cold wall and at the half party of the down wall which is conductive and diffusive at the same time. When N=1, all the kind of entropies generation are located at the top and down corner of the cold wall. When N=2, thermal and solutal entropies become close to the cold wall and to the top wall. Entropy due to the friction increases when the flow is solutal dominated this shows the increase of the viscous irreversibility by the increase of the buoyancyratio.

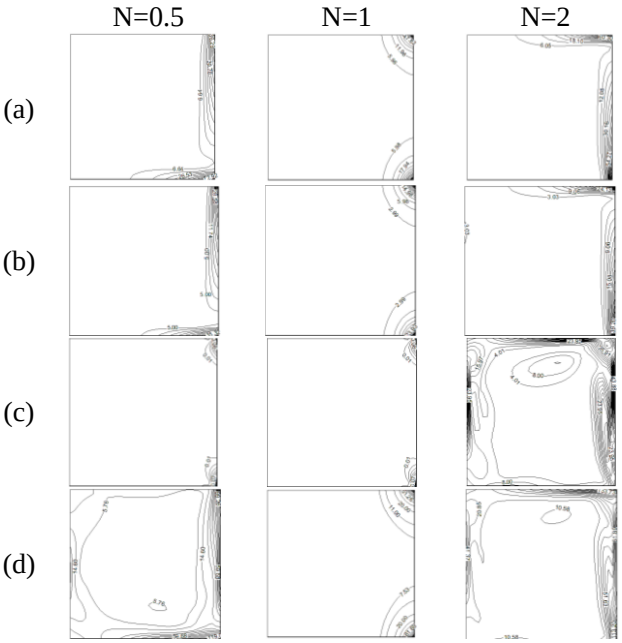

Figure 10. Entropies generation in the XY plan for different N when the boundary condition are diffusive and conductive; (a) thermal , (b) compositional; (c) friction and (d) total

The variations of the mean Bejan number as function of N (figure11) shows that the maximum values of Bejan numbers are detected for the mixed boundary conditions regardless the buoyancy ratio.

For N=1 this variation presents a peak indicating a maximal domination of the heat and mass transfers irreversibility. Bejan number is equal to 0.99 this shows that the heat and mass transfer irreversibility are dominating those due to the flow friction.

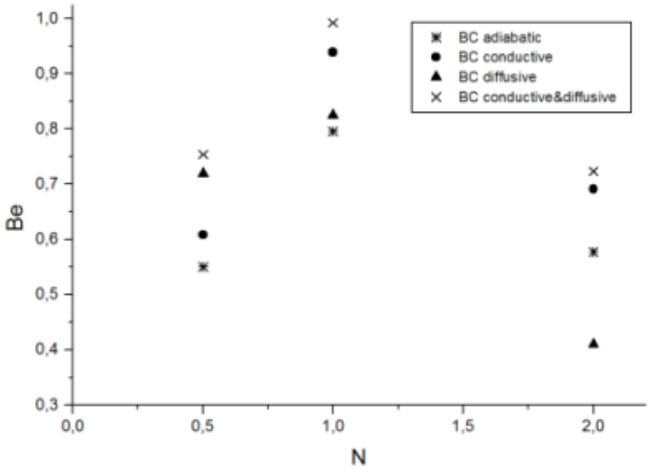

Figure 11. Effect of Boundary condition on the Bejan number for different N

5. Conclusion

Numerical analysis of double diffusive natural convection and entropy generation in three-dimensional cavity is performed in this study. Some conclusions can be drawn:

By the modification of the boundary conditions the transition of flow between thermal and solutal dominated takes place for different values of the buoyancy ratio.

The maximum values of thermal entropy are detected for all tested N values when the boundary conditions are: conductive or simultaneously conductive and diffusive. Nevertheless, the maximum values of diffusive entropy are detected for N=0.5 and N=1 when the boundary condition is diffusive or simultaneously diffusive and conductive. When N=2, the maximum values are detected for conductive boundary condition or for diffusive boundary condition.

Finally, the maximum of Bejan number is detected for N=1 when the boundary condition are simultaneously conductive and diffusive. In fact, Bejan number reaches 0.99 and the thermal and diffusive irreversibility dominate the friction irreversibility.

5. References

[1] De Vahl Davis, G., Natural convection of air in a square cavity: a benchmark numerical solution. Int. J. Numer. Methods Fluids 3, 249–264, 1983.

[2] Bejan, Convection Heat Transfer, 2nd ed., Wiley, New York, 1984.

[3] D. M. Kim and R. Viskanta, Study of the Effects of Wall Conductance on Natural Convection in Differentially Oriented Square Cavities, J. Fluid Mech., vol. 144, pp. 153–176, 1984.

[4] Kim, D.M., Viskanta, R., Effect of wall heat conduction on natural convection heat transfer in a square enclosure. ASME J. Heat transfer 107, 139–146, 1985.

[5] Acharya, S., Tsang, C.H, Influence of wall conduction on natural convection inan inclined square enclosure. Warme- und Stoffubertragung 21, 19–30, 1987.

[6] J. Lee, M. T. Hyun, and K. W. Kim, Natural Convection in Confined Fluids with Combined Horizontal Temperature and Concentration Gradients, Int. J. Heat Mass Transfer, vol. 31, pp. 1969–1977, 1988.

[7] Y. Le Pentrec and G. Lauriat, Effects of the Heat Transfer at the Side Walls on Natural Convection in Cavities, J. Heat Transfer, vol. 112, pp. 370–378, 1990.

[8] T. Fusegi, J. M. Hyun, K. Kuwahara, and B. Farouk, A Numerical Study of 3D Natural Convection in a Cube: Effects of the Horizontal Thermal Boundary Conditions, Fluid Dynam. Res., vol. 8, pp. 221–230, 1991.

[9] J. W. Lee and J. M. Hyun, Time-Dependent Double Diffusion in a Stably Stratified Fluid under Lateral Heating, Int. J. Heat Mass Transfer, vol. 34, pp. 2409–2421, 1991.

[10] C. Beghein, F. Haghighat, and F. Allard, Numerical Study of Double-Diffusive NaturalConvection in a Square Cavity, Int. J. Heat Mass Transfer, vol. 35, pp. 833–846, 1992.

[11] K. Kamakura and H. Ozoe, Experimental and Numerical Analysis of Double Diffusive Natural Convection Heated and Cooled from Opposed Vertical Walls with an Initial Condition of a Vertically Linear Concentration Gradient, Int. J. Heat Mass Transfer, vol. 36,pp. 2125–2134, 1993.

[12] V. A. F. Costa, Double Diffusive Natural Convection in a Square Enclosure with Heat and Mass Diffusive Walls, Int. J. Heat Mass Transfer, vol. 40, pp. 4061–4071, 1997.

[13] T. Nishimura, M. Wakamatsu, and A. M. Morega, Oscillatory Double-Diffusive Convection in a Rectangular Enclosure with Combined Horizontal Temperature and Concentration Gradients, Int. J. Heat Mass Transfer, vol. 41, pp. 1601–1611, 1998.

[14] E. Leonardi, T. A. Kowalewski, V. Timchenko, and G. De Vahl Davis, Effects ofFinite Wall Conductivity on Flow Structures in Natural Convection, Proc. Int. Conf. on Computational Heat and Mass Transfer CHMT, Cyprus, pp. 182–188, 1999.

[15] I. Sezai and A. A. Mohamad, Double Diffusive Convection in a Cubic Enclosure with Opposing Temperature and Concentration Gradient, Phys. Fluids, vol. 12, pp. 2210-2223,2000.

[16] A. Abidi, L. Kolsi, M. N. Borjini, H. Ben Aissia, and M. J. Safi, effect of heat and mass transfer through diffusive walls on three-dimensional double-diffusive natural convection, Numerical Heat Transfer, Part A, 53: 1357–1376, 2008.

[17] Mobedi, M., Conjugate natural convection in a square cavity with finite thickness horizontal walls. Int. J. Commun. Heat Mass Transfer 35, 503–513, 2008.

[18] K. Ghachem, L. Kolsi, Ch.Mâatki, A. K. Hussein, M.N. Borjini, Three-dimensional double diffusive free convection and irreversibilities studies in a solar distiller, International Communications in Heat and Mass Transfer, Volume 39, Issue 6, Pages 869-876, 2012